

Original Article

Cite this article: Rosa D, Gago M, Fernandez-Carvalho J, Coelho R (2021). Life history parameters of the crocodile shark, *Pseudocarcharias kamoharai*, in the tropical Atlantic Ocean. *Journal of the Marine Biological Association of the United Kingdom* **101**, 753–763. <https://doi.org/10.1017/S0025315421000588>

Received: 25 January 2021

Revised: 20 July 2021

Accepted: 26 July 2021

First published online: 18 August 2021


Key words:

Bycatch; elasmobranchs; growth modelling; morphometrics; reproduction

Author for correspondence:

Daniela Rosa, E-mail: daniela.rosa@ipma.pt

Life history parameters of the crocodile shark, *Pseudocarcharias kamoharai*, in the tropical Atlantic Ocean

Daniela Rosa^{1,2} , Marco Gago², Joana Fernandez-Carvalho^{1,2} and Rui Coelho^{1,2}

¹IPMA – Instituto Português do Mar e da Atmosfera, Av. 5 de Outubro s/n, Olhão 8700-305, Portugal and ²CCMAR – Centro de Ciências do Mar, Universidade do Algarve, Campus de Gambelas, Faro 8005-139, Portugal

Abstract

The crocodile shark (*Pseudocarcharias kamoharai*) is a small lamniform shark that is occasionally by-caught in pelagic longline fisheries targeting tunas and swordfish. Due to its biological features, this species is highly vulnerable to overexploitation. However, at present, the crocodile shark is not evaluated for its stock status by any of the Regional Fisheries Management Organizations. In this study, the biology of 391 specimens (220 females and 171 males), ranging from 44.2 cm to 101.5 cm fork length (FL), collected from the tropical region of the Atlantic Ocean, was examined. Ages were assigned from growth band counts in vertebral sections, with the modified von Bertalanffy growth model, using a fixed size at birth (L_0) at 32 cm FL, producing the best fit: $L_{inf} = 105.6$ cm FL and $k = 0.14$ y^{-1} for females; $L_{inf} = 94.6$ cm FL and $k = 0.18$ y^{-1} for males. Maturity ogives were fitted to both length- and age-based data. The size (L_{50}) and age (A_{50}) at 50% maturity was estimated at 67.2 cm FL (5 years) and 81.6 cm FL (8 years) for males and females, respectively. Mean uterine fecundity was 3.7 pups per litter with a 1:1 embryonic sex ratio. Further work is needed regarding crocodile shark life-history characteristics, especially because there are no age validation studies of the band pair deposition periodicity. However, the parameters now presented can contribute to future evaluations of this species, which is especially important given its potentially vulnerable life history.

Introduction

The crocodile shark, *Pseudocarcharias kamoharai*, is a small-sized oceanic pelagic shark belonging to the order Lamniformes. It is the smallest lamniform species with a size at birth of around 41 cm total length (Oliveira *et al.*, 2010) and the only species of the family Pseudocarchariidae. The crocodile shark has an epipelagic and mesopelagic circumtropical distribution, it is usually found offshore and far from land but sometimes occurs inshore (Compagno, 2001). Vertically it can be distributed at depths from the surface to at least 590 m (Compagno, 2001). Despite being caught in tropical and sub-tropical waters in the Atlantic, Indian and Pacific oceans, the crocodile shark has an apparent unequal distribution, as in some regions it is quite rare while in others can be relatively abundant (Compagno, 2001).

Pseudocarcharias kamoharai is occasionally caught as by-catch by longliners targeting tuna and swordfish (Hazin *et al.*, 1990). In the Portuguese longline fishery, the crocodile shark is more captured in some of the fishing areas, such as around the Cabo Verde archipelago and in the Gulf of Guinea, albeit in much lower numbers than the blue shark (*Prionace glauca*) (Coelho *et al.*, 2012). Caught individuals are usually discarded, dead or alive, due to its lack of commercial value (Oliveira *et al.*, 2010). Therefore, this species is not accounted for in the official fisheries landings statistics, limiting the availability of data for monitoring its fisheries mortality and assessing its population status.

Elasmobranchs are, in general, highly susceptible to overexploitation due to their life history characteristics (Stevens *et al.*, 2000). Lamniform sharks are even more susceptible due to their low fecundity, and specifically in the crocodile shark usually only four individuals are born per female in each reproductive cycle (Oliveira *et al.*, 2010; Dai *et al.*, 2012). The crocodile shark is globally listed as 'Least Concern' by the IUCN Red List criteria (Kyne *et al.*, 2019), however it is noted that catch rates and population trends should continue to be monitored due to its vulnerability as by-catch in longline fisheries and due to its life history traits (Kyne *et al.*, 2019). In 2012, Cortés *et al.* (2015) conducted an ecological risk assessment (ERA) for several elasmobranch species in the Atlantic, and while the crocodile shark was initially considered for this analysis, the lack of biological data hampered the assessment.

A few studies of crocodile shark reproduction have been carried out in the Pacific (Fujita, 1981; Dai *et al.*, 2012), Indian (White, 2007) and Atlantic (Oliveira *et al.*, 2010; Wu *et al.*, 2020) oceans. Since the Cortés *et al.* (2015) ERA, two age and growth studies have become available for this species in the Atlantic Ocean (Lessa *et al.*, 2016; Kindong *et al.*, 2020). Age and growth studies are fundamental to estimate population growth rates, natural mortality, and longevity of a species (Campana, 2001).



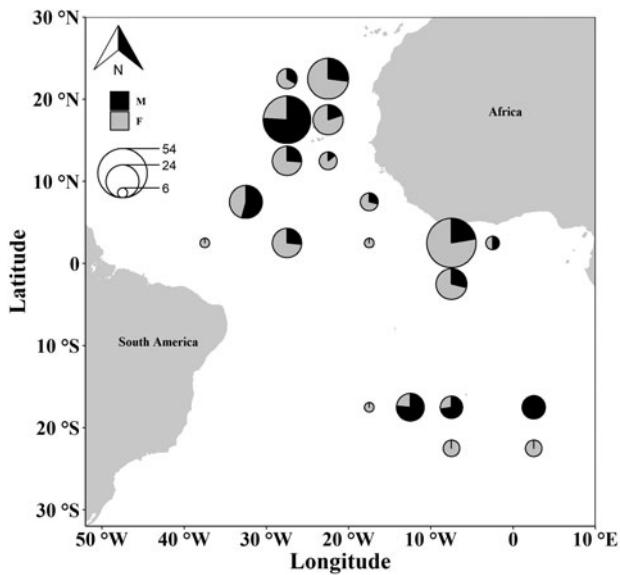


Fig. 1. Map of the Atlantic areas with the sampling locations of the crocodile shark (*Pseudocarcharias kamoharai*). The circles are represented in a 5° × 5° grid, with the sizes of the circles proportional to sample size and colour representing sex.

To add to the knowledge of the vital life-history parameters of this species, the objectives of this work were to study various aspects of the life history parameters of *P. kamoharai*, specifically growth, maturity and fecundity. The results presented here will be useful for modelling purposes (e.g. risk analysis) and may serve as a basis for comparison with other studies on this species, both in the Atlantic as well as in other oceans.

Materials and methods

Biological samples

Specimens were obtained by observers from the Portuguese Institute for the Ocean and Atmosphere (IPMA, I.P.) on board Portuguese commercial longline vessels targeting swordfish between 2009 and 2012. Samples were collected over a wide Atlantic region (latitudes 25°N to 25°S; longitudes 7°E to 40°W) (Figure 1).

All specimens caught were frozen onboard, brought to the laboratory and processed shortly after. Each specimen was sexed, and a series of external body measurements were taken to the nearest lower centimetre, namely the total length (TL), measured in a straight line from the tip of the snout to the tip of the caudal fin in its natural position, the fork length (FL), measured from the tip of the snout to the caudal fin fork, and the pre-caudal length (PCL), measured from the tip of the snout to the beginning of the upper lobe of the caudal fin. Total weight (W) and eviscerated weight (Wev) were recorded to the nearest centigram. After dissection, the liver was weighed to the nearest centigram. For females, the oviducal glands and uteri were measured for width and the ovary measured for width and length and weighed. Following dissection, the contents of the uteri were observed, and any developing embryos were counted and sexed. For males, the testes were measured for width and length, and weighed, the claspers were measured for inner and outer length and the presence of semen in the seminal glands recorded. All organs were measured to the nearest 0.1 mm using a digital calliper and weighed on a digital scale with a 0.01 g precision. The sex ratio of the samples was calculated and tested for equal proportions with a chi-square test.

Morphometric relationships

The length-length relationships between TL, PCL and FL and the length-weight relationship between FL, W and Wev without any

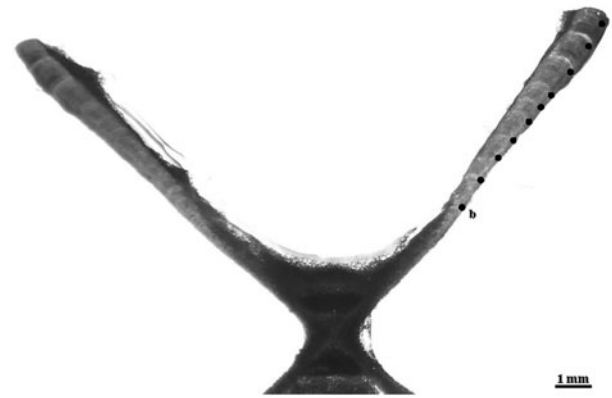


Fig. 2. Microphotograph of a vertebral section of the crocodile shark (*Pseudocarcharias kamoharai*), from a female specimen with 80 cm fork length with the identification of the birth mark (b) and the estimated nine growth bands.

data transformation, and the weight-weight relationship between W and Wev (in g) with natural logarithm transformed data were explored by linear regression. Standard errors were calculated for all the estimated parameters, along with the coefficient of determination (r^2) of each regression. Linear regressions were carried out to compare the main effects of the explanatory variable and sex and the interaction term between the explanatory variable and sex.

Age estimation and validation

A section of 3–5 vertebrae was extracted from the region below the anterior part of the first dorsal fin. The covering of connective tissue on the vertebrae was first removed with scalpels, and then by soaking the vertebrae in 4–6% sodium hypochlorite (commercial bleach) for 5 to 10 min, depending on size. Once cleaned, the vertebrae were stored in 70% ethanol and then air-dried for 24 h before embedding in polyester resin, in individual plastic moulds, and left to harden for ~24 h.

The resin blocks with the embedded vertebrae were sectioned sagittally with a Buehler Isomet (Lake Bluff, IL) low-speed saw, using two blades spaced ~500 μ m apart. The resulting section included the focus of the vertebra and the two halves (one on each side of the focus), in a form typically called 'bow-tie'. Finally, the sections were stained with crystal violet (Sigma-Aldrich Co., St. Louis, MO). Once dried, the sections were mounted onto microscope slides with Cytoseal 60 (Thermo Fisher Scientific Inc., Waltham, MA). The visualization of the vertebral sections was carried out under a dissecting microscope using transmitted white light (Figure 2).

Sections from the same specimen were read once by two different readers. Counts were made with no knowledge of the sex or size of the individual. Whenever band pair counts differed between the two readers by one or two band pairs, a third reading was made. If disagreement between readings persisted or if the band pair count between readers disagreed by three or more band pairs, the section was discarded. The precision of the age estimates was determined by several different techniques. The per cent agreement (PA), the average per cent error (APE) defined by Beamish & Fournier (1981) and the coefficient of variation (CV) were used. Bias plots were used to graphically assess the ageing accuracy between the readers (Campana, 2001). Precision analysis was carried out using the R language for statistical computing version 3.6.1 (R Core Team, 2019), using the package 'FSA' (Ogle et al., 2020). All plots were performed using package 'ggplot2' (Wickham, 2016).

Table 1. Morphometric relationships for crocodile shark (*Pseudocarcharias kamoharui*) collected in the tropical Atlantic Ocean

Relationship	Sex	Sample characteristics		Parameters of the relationship				
		N	Range	<i>a</i>	SE <i>a</i>	<i>b</i>	SE <i>b</i>	<i>r</i> ²
TL-FL	Combined	380	44.2–101.5	5.18	0.96	1.11	0.01	0.96
	Males	163	44.2–92.8	6.78	1.66	1.09	0.02	0.95
	Females	217	57.0–101.5	3.71	1.16	1.13	0.01	0.97
TL-PCL	Combined	380	42.2–91.5	6.81	1.03	1.21	0.01	0.95
	Males	163	42.2–84.5	8.06	1.83	1.20	0.03	0.93
	Females	217	50.0–91.5	5.38	1.21	1.22	0.02	0.96
FL-PCL	Combined	386	42.2–91.5	2.81	0.84	1.07	0.01	0.96
	Males	168	42.2–84.5	2.97	1.47	1.07	0.02	0.94
	Females	218	50.0–91.5	2.60	1.00	1.08	0.01	0.97
W-Wev	Combined	382	675–7150	235.50	30.5	0.64	0.01	0.93
	Males	167	675–4935	109.22	35.32	0.70	0.01	0.96
	Females	215	1210.0–7150.0	211.09	43.26	0.63	0.01	0.93
W-FL	Combined	385	44.2–101.5	−5.46	0.30	3.07	0.07	0.84
	Males	169	44.2–92.8	−4.94	0.37	2.94	0.08	0.88
	Females	216	57.0–101.5	−5.54	0.44	3.09	0.10	0.82
Wev-FL	Combined	380	44.2–101.5	−5.20	0.26	2.93	0.06	0.87
	Males	166	44.2–92.8	−5.31	0.36	2.96	0.08	0.89
	Females	214	57.0–101.5	−5.07	0.37	2.91	0.09	0.84

For each model, parameters are presented with the respective standard errors (SE) and the coefficient of determination (r^2). TL = total length (cm), FL = fork length (cm), PCL = pre-caudal length (cm), W = total weight (g), Wev = Eviscerated weight (g). Range is in centimetres for the length-length and length-weight relationships, and in grams for the weight-weight relationship. Length-length and weight-weight relationships do not have any transformation while length-weight relationships are log transformed.

Growth modelling

The relationship between the size of the specimens and the size of their vertebrae was determined. The vertebral sections were photographed using a dissecting microscope and the vertebral radius of the vertebrae was digitally measured using Image J software (Abramoff *et al.*, 2004). A linear and a quadratic regression was fitted using FL as the dependent variable and the vertebral radius (VR) as the independent variable. Model comparison was based on Akaike information criterion (AIC) and Bayesian information criterion (BIC) and the coefficient of determination (r^2), where the model with the lowest AIC/BIC and highest r^2 was considered the model that best fitted the data and described the FL-VR relationship.

To verify the temporal periodicity of band formation in the vertebral centra, an edge analysis and a marginal increment analysis was initially attempted. However, due to the lack of captures for each month and for every estimated age class, it was not possible to determine the periodicity of band formation. The deposition of a band pair (one translucent and one opaque band) per year was assumed (see Discussion section for details).

Five models were used to describe this species' growth. The 3-parameter von Bertalanffy growth function (VBGF) re-parameterized to estimate L_0 (size at birth) instead of t_0 (theoretical age at which the expected length is zero), as suggested by Cailliet *et al.* (2006):

$$L_t = L_{\text{inf}} - (L_{\text{inf}} - L_0) \times \exp^{-k_1 \times t} \quad (1)$$

A 2-parameter VBGF where L_0 was fixed to the size at birth described for this species was also used.

The Gompertz growth function (GOM):

$$L_t = L_{\text{inf}} \times \exp^{-a \times \exp^{-k_2 \times t}} \quad (2)$$

The logistic model (LOG):

$$L_t = \frac{L_{\text{inf}}}{1 + \exp^{-k_3 \times (t - t_i)}} \quad (3)$$

Finally, a Richards model (RICH) re-parameterized to estimate L_0 was also used, with a fixed L_0 at the size at birth described for this species:

$$L_t = L_{\text{inf}} \times \left(1 + \left(\frac{L_0}{L_{\text{inf}}}^{(1-b)} - 1 \right) \times \exp^{-k_4 \times t} \right)^{1/(1-b)} \quad (4)$$

where L_t = mean fork length at age t ; L_{inf} = mean asymptotic fork length; k_1 = relative growth coefficient; L_0 = fork length at birth; k_2 = instantaneous growth rate at the inflection point; a = dimensionless parameter related to growth; k_3 = instantaneous growth rate at negative infinity; t_i = time at the inflection point; k_4 = controls the slope at the inflection point; b = a dimensionless parameter that controls the vertical position of the inflection point.

For the models with fixed L_0 , because size data in our study refer to FL, the size at birth from Oliveira *et al.* (2010) of 41 cm TL was converted using the TL-FL relationship in Table 1, resulting in 32 cm FL.

Model comparison was based on AIC and BIC. Growth models were fitted using non-linear least squares function from the 'minpack.lm' package (Elzhov *et al.*, 2016) in R (R Core Team, 2019). A likelihood ratio test (LRT) was used to test the null

hypothesis that there was no difference in growth parameters between males and females.

Maturity and fecundity

Maturity was assigned by macroscopically observing the condition of the reproductive system. Following Oliveira *et al.* (2010), for males, maturity was assigned based on the calcification and size of the claspers; for females, maturity was assigned based on the presence of uterine contents and the dimensions of the reproductive organs such as the ovary, oviducal glands, and uterus. For paired structures, both the left- and the right-side structures were measured and tested for normality with Kolmogorov–Smirnov normality tests with the Lilliefors correction (Lilliefors, 1967), and for homogeneity of variances with Levene tests (Levene, 1960). Dimensions of the structures was compared among left and right side using non-parametric 2-sample permutation tests (Manly, 2007). Each structure dimension, for each male and female, was plotted against FL so that relative growth of the structure with size could be observed (Supplementary material).

The gonadosomatic index (GSI) and the hepatosomatic index (HSI) were calculated as:

$$\text{GSI} = \frac{\text{Gonad weight(g)}}{\text{Wew(g)}} \times 100 \quad (5)$$

$$\text{HSI} = \frac{\text{Liver weight(g)}}{\text{Wew(g)}} \times 100 \quad (6)$$

For males, gonad weight was calculated as the sum of left and right testis weight, for females the ovary weight was used. GSI and HSI was tested for normality with Kolmogorov–Smirnov normality tests with the Lilliefors correction (Lilliefors, 1967), and for homogeneity of variances with Levene tests (Levene, 1960). To test for differences in GSI and HSI between mature and immature specimens, ANOVA tests were performed. When the assumptions of parametric tests were not met, non-parametric 2-sample permutation tests (Manly, 2007) were used. A plot of HSI and GSI for mature specimens was produced for visual inspection of the monthly trends in these indices.

Raw maturity data were used to fit length-based maturity ogives and to estimate the size at 50% maturity (L_{50} , FL at which 50% of the individuals are mature). A logistic regression was fit by GLM with a binomial response variable, using the 'glm' function in R (R Core Team, 2019). The predicted probability of an individual being mature at a given length is given by:

$$P_{L_i} = \frac{\exp(\alpha + \beta \times L_i)}{1 + \exp(\alpha + \beta \times L_i)} \quad (7)$$

where P_{L_i} is the probability of an individual being mature at length i , α the intercept term and β the effect size in terms of length.

The same procedure was followed to fit age-based maturity ogives and estimate age at maturity (A_{50} , age at which 50% of the individuals are mature). The predicted probability of an individual being mature at a given age is given using the equation:

$$P_{\text{Age}_i} = \frac{\exp(\alpha + \beta \times \text{Age}_i)}{1 + \exp(\alpha + \beta \times \text{Age}_i)} \quad (8)$$

where P_{Age_i} is the probability of an individual being mature at age i , α the intercept term and β the effect size in terms of age.

The inflection points of the relationships represent L_{50} and A_{50} , where $P=0.5$, these values were calculated and 95%

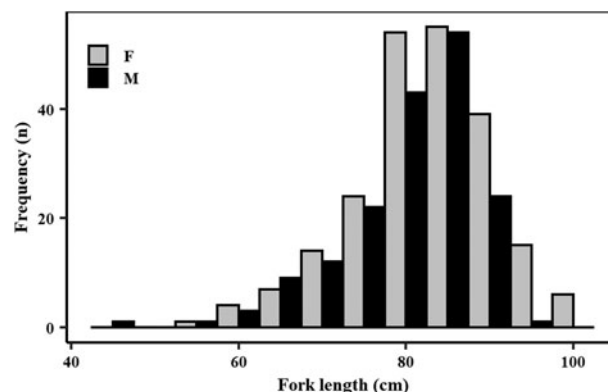


Fig. 3. Length (fork length, in 5 cm length bins) frequency distribution of male (N=171) and female (N=220) crocodile shark (*Pseudocarcharias kamoharai*), collected in the tropical Atlantic Ocean.

confidence intervals (CI) obtained through bootstrapping from binomial GLM fits to 1000 resamples of the maturity data using the 'boot' package (Canty & Ripley, 2019). Length and age-based maturity ogives were fitted to males and females separately, and an LRT used to test for differences between sexes.

Fecundity was estimated by direct methods, by counting the number of mid-term embryos in pregnant females. Numbers of developing embryos occurring in the left and right uteri were compared with a Mann–Whitney U-test (given that the samples were not normally distributed). The sex ratio of the embryos was calculated and tested for equal proportions with a chi-square test.

Results

Biological samples

A total of 391 specimens (220 females and 171 males) was caught for this study during the sampling period. The sex ratio of the samples significantly favoured females (two proportion z-test, $n_{\text{females}} = 220$, $n_{\text{males}} = 171$, $\chi^2 = 12.28$, $P < 0.001$). Of these samples, 358 specimens were used for the age and growth study and 387 specimens for the maturity component. Both male and female samples had a wide length range (Figure 3), covering most of the length range described for this species. Females attained slightly larger sizes than males. Specifically, female lengths varied from 57.0–101.5 cm FL while males ranged from 44.2–92.8 cm FL (Figure 3). Males ranged in total weight from 675–5120 g and females from 1210–7425 g.

Morphometric relationships

The morphometric relationships for *P. kamoharai* are presented in Table 1. For the TL-FL relationship the interaction term between FL and sex was not significant and no significant differences between sexes were detected (ANOVA_{FL:Sex}: $F = 2.02$, $P > 0.05$; ANOVA_{Sex}: $F = 2.09$, $P > 0.05$). For TL-PCL there is not a significant interaction term between PCL and sex (ANOVA_{PCL:Sex}: $F = 1.12$, $P > 0.05$) but significant differences were found for sex (ANOVA_{Sex}: $F = 4.33$, $P < 0.05$), this means that the slope of the regression curve is not significantly different between the sexes, but the intercept between sexes is different. For the FL-PCL relationship, the interaction term between PCL and sex was not significant and no significant differences between sexes were detected (ANOVA_{PCL:Sex}: $F = 0.03$, $P > 0.05$; ANOVA_{Sex}: $F = 0.21$, $P > 0.05$).

For the W-Wev regression a significant interaction was found between Wev and sex and significant differences were detected

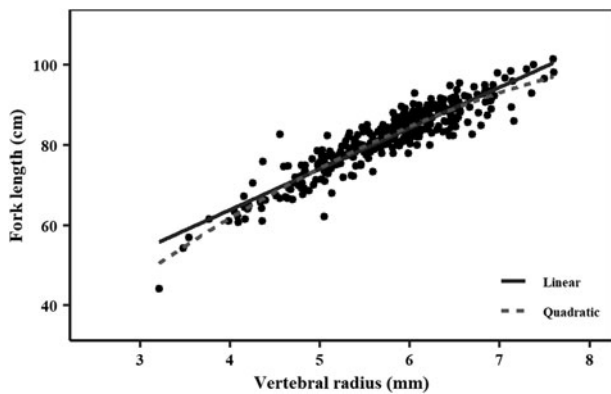


Fig. 4. Relationship between fork length (cm) and vertebrae centrum radius (mm) for crocodile shark (*Pseudocarcharias kamoharai*) collected in the tropical Atlantic Ocean. Dots represent individual observations. Solid line represents linear regression where: $FL = 23.03 + 10.20 \times VR$. Dashed line represents quadratic regression where: $FL = 21.75 \times VR - 1.03 \times VR^2 - 8.76$. FL = fork length; VR = vertebral radius.

between sexes (W-Wev: $ANOVA_{Wev:Sex}: F = 14.78, P < 0.001$; $ANOVA_{Sex}: F = 43.99, P < 0.001$). For W-FL the interaction term between FL and sex was not significant but significant differences between sexes were detected ($ANOVA_{TL:Sex}: F = 1.30, P > 0.05$; $ANOVA_{Sex}: F = 25.69, P < 0.001$), whereby females are significantly heavier than males for a given length. For Wev-FL the interaction term between FL and sex was not significant and no significant differences between sexes were detected ($ANOVA_{FL:Sex}: F = 0.19, P > 0.05$; $ANOVA_{Sex}: F = 0.91, P > 0.05$).

Age estimation and growth modelling

There was a slight curvilinear relationship between VR and FL (Figure 4). A linear regression had a good fit to the data ($FL = 23.03 + 10.20 \times VR$; $r^2 = 0.85$; AIC = 1830; BIC = 1842); however, the quadratic equation produced a slightly better goodness-of-fit ($FL = 21.75 \times VR - 1.03 \times VR^2 - 8.76$; $r^2 = 0.86$; AIC = 1806; BIC = 1822). Inter-specific CV and APE were 5.61% and 3.97%, respectively. PA between the first and second reader was 48.01%, while the PA within one and two band pairs was 89.49% and 97.73%, respectively. A high agreement with no systematic bias was observed between the readings of the two readers using the age-bias plots (Figure 5).

A total of 338 (94.41%) vertebrae had a final agreed band pair count and thus were accepted for growth modelling. Fork lengths

of individuals with an agreed band pair count ranged from 57.0–100.0 cm and 44.2–92.8 cm FL for females and males, respectively. Estimated ages of the analysed specimens ranged from 3–14 years for females and from 2–13 years for males. The LRT revealed significant differences between males and females for all growth models (LRT; 3-parameter VBGF: $\chi^2 = 32.06, df = 3, P < 0.001$; 2-parameter VBGF: $\chi^2 = 31.15, df = 2, P < 0.001$; GOM: $\chi^2 = 32.02, df = 3, P < 0.001$; LOG: $\chi^2 = 31.95, df = 3, P < 0.001$; RICH: $\chi^2 = 31.94, df = 3, P < 0.001$), therefore growth models were calculated for each sex separately.

All five models produced very similar curves, both in the case of males and females (Figure 6). AIC values were similar, despite VBGF with a fixed L_0 having the lowest AIC, for both females and males, BIC presents the same tendency, with differences between the VBGF with a fixed L_0 being larger than for AIC (Table 2). In general, the differences between the AIC/BIC values are small, indicating that there is little statistical difference between the models.

In all models, females had higher maximum asymptotic sizes than males. The logistic equation produced the lowest maximum asymptotic lengths and the VBGF with a fixed L_0 the highest values, inversely the estimated growth coefficients were lower for the VBGF with a fixed L_0 and highest for the logistic model (Table 2, Figure 6). The VBGF estimated L_0 of 20.6 cm FL for males and 22.9 cm FL for females are smaller than the reported size at birth for this species.

Maturity and fecundity

In the case of males, HSI data were not normally distributed (Lilliefors test: $D = 0.09, P < 0.001$), but the variances were homogeneous between mature and immature individuals (Levene test: $F = 0.19, df = 1, P > 0.05$). Using univariate non-parametric statistical tests revealed that HSI did not differ significantly between mature and immature individuals (permutation test: $Z = 1.13, P > 0.05$; Figure 7). GSI data were not normally distributed (Lilliefors test: $D = 0.12, P < 0.001$), and the variances were heterogeneous between mature and immature individuals (Levene test: $F = 12.34, df = 1, P < 0.001$). Using univariate non-parametric statistical tests revealed that GSI did not differ significantly between mature and immature individuals (permutation test: $Z = 0.25, P > 0.05$; Figure 7). For females, HSI data were normally distributed (Lilliefors test: $D = 0.05, P > 0.05$), and the variances were homogeneous between mature and immature individuals (Levene test:

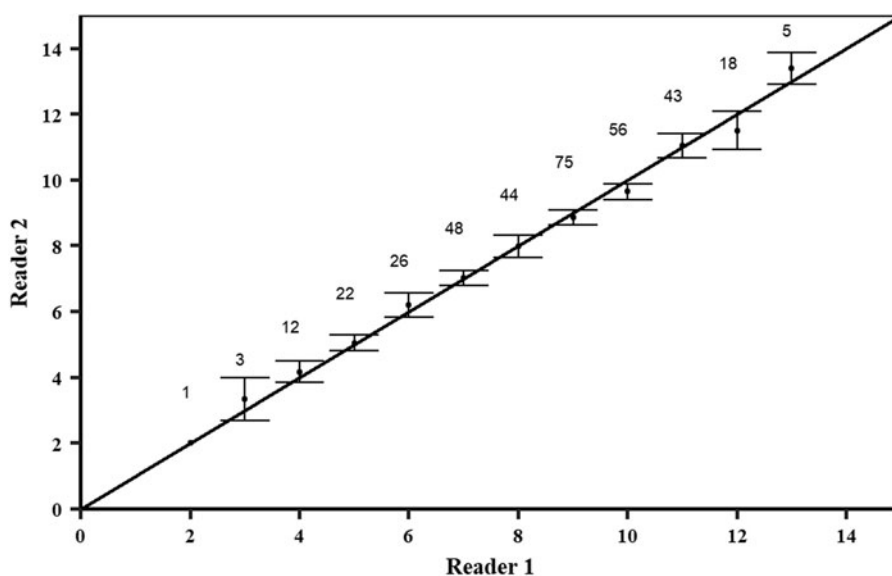


Fig. 5. Age-bias plots of pairwise growth band counts comparisons between reader 1 and reader 2. Numbers represent number of samples and dots with error bars represent the mean counts of reading (\pm 95% confidence intervals) relative to the accepted growth band count. The diagonal line indicates a one-to-one relationship.

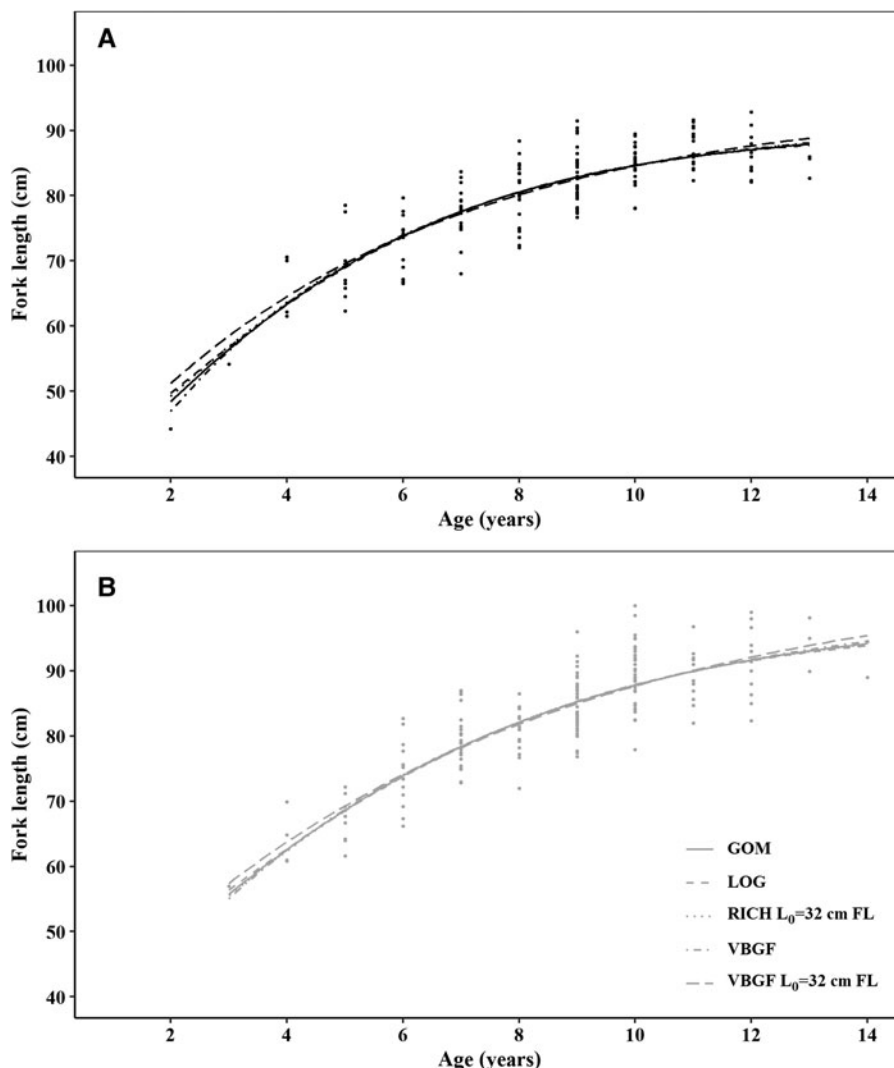


Fig. 6. Growth functions for (A) males and (B) females crocodile shark (*Pseudocarcharias kamoharui*) in the tropical Atlantic, based on growth band counts in vertebral sections. Circles represent observed data and lines represent the fitted models. VBGF stands for the von Bertalanffy growth function, VBGF $L_0 = 32$ cm FL for the VBGF with fixed size at birth at 32 cm fork length GOM for the Gompertz model, LOG for the logistic model and RICH $L_0 = 32$ cm FL for the Richards model with fixed size at birth at 32 cm fork length.

$F = 0.45$, $df = 1$, $P > 0.05$). Differences were found between stages for female HSI (ANOVA: $F = 3.98$, $P < 0.05$), with mature females having a higher HSI (Figure 7). GSI data were not normally distributed (Lilliefors test: $D = 0.39$, $P < 0.001$), and the variances were heterogeneous between mature and immature individuals (Levene test: $F = 38.65$, $df = 1$, $P < 0.001$). Using univariate non-parametric statistical tests revealed that GSI significantly differed between stages for females (permutation test: $Z = 5.89$, $P < 0.001$), with mature females having a higher GSI (Figure 7).

Although with limited sample size by month and some missing months, a graphic representation of the HSI and GSI for mature specimens by month shows that there is low variation in HSI through the year for males (Figure 7) while for females there is a small decrease in the months where GSI is higher (Figure 7). For males, in the months from April to September the GSI also shows an increasing trend when compared with the other available months (Figure 7).

Immature males in the sample ranged from 44.2–77.6 cm FL, while mature males ranged from 62.2–92.8 cm FL, with 157 out of 169 (92.9%) of the males in the sample being mature. Immature females ranged from 57–93.7 cm FL, with the smallest mature female measuring 75.5 cm FL, and with 120 out of 218 (55.0%) of the females being mature. In terms of age, the youngest mature male was 4 years old, while the oldest immature male was 9 years old. Females matured at a later age, with the youngest mature female being 6 years old and the oldest immature female being 11 years old.

Females matured at larger sizes than males, with estimated L_{50} of 81.57 cm FL for females and 67.20 cm FL for males (Figure 8,

Table 3). Females also matured at later ages than males, with estimated A_{50} of 4.85 years for males and 8.21 years for females (Figure 8, Table 3). There were significant differences between sexes in terms of the parameters of both length (LRT: $\chi^2 = 149.88$, $df = 2$, $P < 0.05$) and age-based (LRT: $\chi^2 = 103.03$, $df = 2$, $P < 0.05$) maturity ogives.

Pregnant females were found in February, March, May, June and December, with most pregnancies occurring in May and June. Uterine fecundity varied from 2–4 embryos with a mean of 3.7 (SD = 0.6, $n_{\text{females}} = 34$, $n_{\text{embryos}} = 123$). No differences were found in the mean number of embryos counted in each uterus (Mann–Whitney U test, $U = 580.5$, $n_{\text{left}} = 61$, $n_{\text{right}} = 62$, $P > 0.05$). Most pregnant females had two embryos in each uterus, although 1 embryo per uterus ($n = 3$) and 2 in one uteri and 1 in the other ($n = 3$) was also found. The sex ratio of the embryos was close to 1:1, but slightly favoured females (53.2% females v. 46.8% males), although no significant statistical difference was detected (two proportion z-test, $n_{\text{females}} = 58$, $n_{\text{males}} = 51$, $\chi^2 = 0.66$, $df = 1$, $P > 0.05$). The most typical situation observed was for a pregnant female to have one male and one female embryo in each uterus, totalling two males and two females per reproductive cycle.

Discussion

Most of the known length range of the species was covered in the present study, namely with the lengths ranging from 44.2–101.5 cm FL, and with females attaining larger sizes than males. At the higher end, the larger individual in this study is close to the maximum reported

Table 2. Growth parameters for crocodile shark (*Pseudocarcharias kamoharui*) from the tropical Atlantic Ocean, fitted with individual observed data

Sex	Model	AIC	BIC	Parameter	Estimate	SE	95% CI	
							Lower	Upper
Males	VBGF	895	907	L_{inf}	91.56	1.95	87.72	95.41
				k	0.23	0.03	0.17	0.3
				L_0	20.61	7.78	5.24	35.99
	VBGF $L_0 = 32$	895	904	L_{inf}	94.55	1.75	91.09	98.01
				k	0.18	0.01	0.16	0.21
	GOM	895	908	L_{inf}	90.4	1.67	87.11	93.7
				k	0.28	0.04	0.21	0.35
				a	1.09	0.14	0.82	1.37
	LOG	896	908	L_{inf}	89.62	1.48	86.69	92.54
				k	0.33	0.04	0.25	0.41
				t_i	1.33	0.32	0.69	1.96
	RICH $L_0 = 32$	895	908	L_{inf}	90.66	2.50	85.72	95.6
				k	0.28	0.08	0.12	0.43
				b	1.09	0.84	-0.57	2.75
	Females	VBGF	1045	1058	L_{inf}	101.14	3.80	93.63
k					0.18	0.03	0.11	0.24
L_0					22.86	8.77	5.55	40.18
VBGF $L_0 = 32$		1044	1054	L_{inf}	105.64	2.75	100.21	111.06
				k	0.14	0.01	0.12	0.16
GOM		1044	1057	L_{inf}	98.75	2.96	92.91	104.58
				k	0.23	0.04	0.16	0.30
				a	1.13	0.13	0.86	1.39
LOG		1044	1057	L_{inf}	97.14	2.45	92.31	101.97
				k	0.28	0.04	0.20	0.35
				t_i	1.82	0.29	1.25	2.4
RICH $L_0 = 32$		1044	1057	L_{inf}	98.14	3.92	90.4	105.87
				k	0.24	0.07	0.09	0.38
				b	1.13	0.8	-0.44	2.7

The presented models are the re-parameterized von Bertalanffy growth function (VBGF), the VBGF with fixed L_0 at 32 cm fork length (FL), the Gompertz growth function (GOM), the logistic model (LOG) and the Richards model (RICH) with fixed L_0 at 32 cm. For each model, parameters are presented with the respective standard errors (SE) and 95% confidence intervals (CI). L_{inf} = mean asymptotic length (cm FL), k_1 = relative growth coefficient (year^{-1}), L_0 = size at birth (cm FL), k_2 = instantaneous growth rate at the inflection point (year^{-1}); a = dimensionless parameter related to growth; k_3 = instantaneous growth rate at negative infinity (year^{-1}); t_i = time at the inflection point (year), k_4 = controls the slope at the inflection point (year^{-1}); b = a dimensionless parameter that controls the vertical position of the inflection point.

length of 105¹ cm FL (122 cm TL; Lessa *et al.*, 2016). Size at birth is reported to be between 36 and 45 cm TL according to White (2007), this range corresponds to 28–36 cm FL, which implies our study missed only the smallest individuals between the size at birth and 44.2 cm FL. Moreover, only a few samples were available below 60 cm FL. The lack of small individuals has also been reported in several studies focusing on crocodile shark life history (e.g. Oliveira *et al.*, 2010; Lessa *et al.*, 2016; Kindong *et al.*, 2020; Wu *et al.*, 2020). Oliveira *et al.* (2010) proposed that the absence of small individuals could be related to size selectivity of the gear or due to the absence of these individuals either due to different geographic distribution or different vertical distribution of the fishing gears compared with the distribution of those smaller specimens.

The sex ratio in the sample was significantly different from the expected 1:1, with more females in the catch as found by several

authors (White, 2007; Oliveira *et al.*, 2010; Dai *et al.*, 2012; Lessa *et al.*, 2016). On the contrary, some studies reported more males than females in fisheries catches (Ariz *et al.*, 2006, 2007; Romanov *et al.*, 2008; Walsh *et al.*, 2009; Kindong *et al.*, 2020). The unbalanced sex ratios in different areas may indicate that fish aggregations can be spatially or temporally dependent (Dai *et al.*, 2012). Sexual segregation and juvenile aggregations in specific areas might lead to a higher vulnerability of crocodile shark to commercial fisheries (Romanov *et al.*, 2008; Dai *et al.*, 2012).

Regarding the precision of age readings, Campana (2001) mentions that precision is highly influenced by the species and the nature of the structure used, reporting that most ageing studies using vertebrae report a CV higher than 10%. In the current study, CVs were low and PA was high, especially within one band pair readings. The precision of age readings with the bias-plot graphics indicates that our age estimates were consistent.

An annual band-pair deposition rate was assumed in this study. An initial attempt to verify band pair deposition through

¹All total lengths were converted to fork lengths using the TL-FL equation in Table 1.

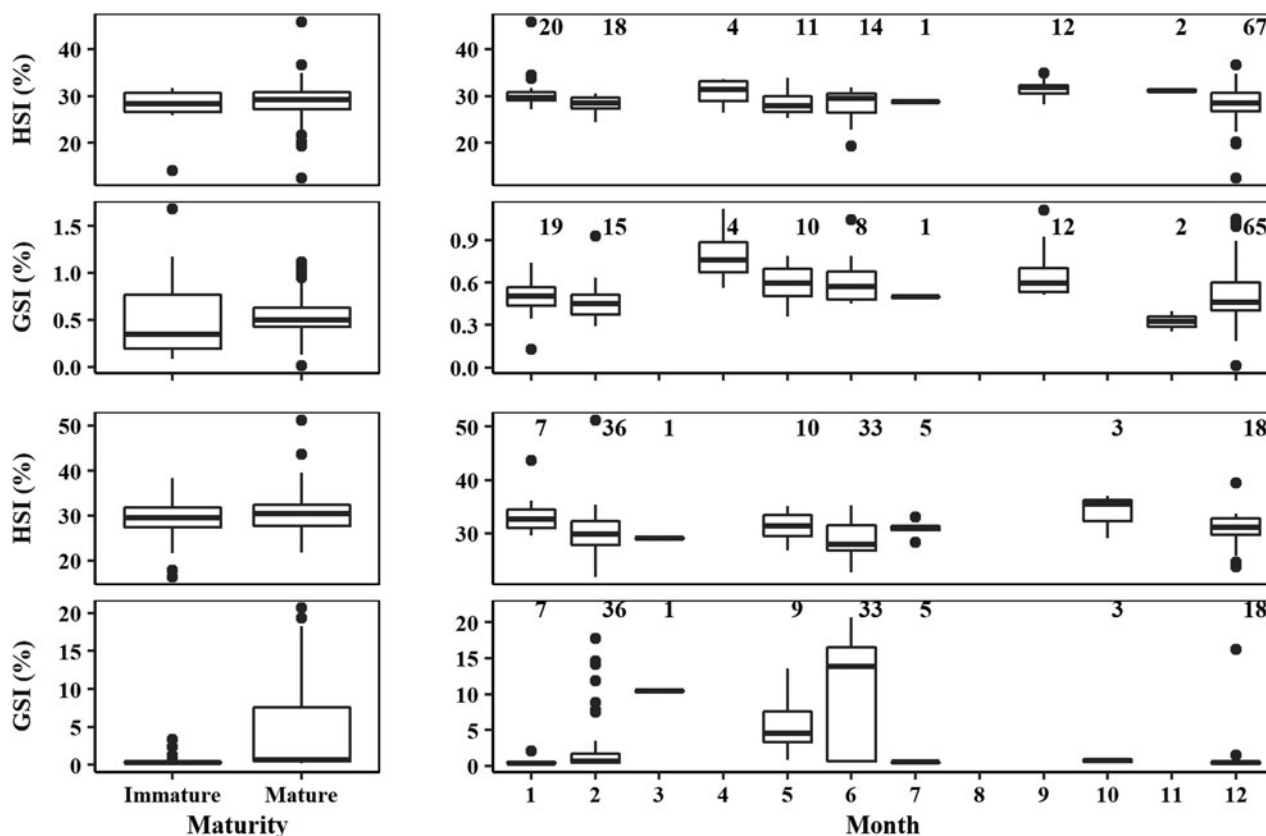


Fig. 7. Boxplot of the hepatosomatic index (HSI, %) and gonadosomatic index (GSI, %) between immature and mature specimens (left) and for mature specimens by month (right) for male (top) and female (bottom) crocodile shark (*Pseudocarcharias kamoharui*) in the tropical Atlantic Ocean. The box corresponds to the interquartile range (IQR, between the 25th and 75th percentiles), whiskers maximum and minimum represent the largest and lowest value, respectively, no further than 1.5*IQR, and dots represent data outside of this range.

marginal increment analysis was performed, however due to a heterogeneous sample size by month it was not possible to conduct this analysis. Lessa *et al.* (2016) conducted a marginal increment analysis but results were inconclusive. Annual band pair deposition has been validated for other species of the same order, for example *Alopias superciliosus* (Liu *et al.*, 1998), *Alopias pelagicus* (Liu *et al.*, 1999), *Lamna nasus* (Natanson *et al.*, 2002) and *Isurus oxyrinchus* (Ardizzone *et al.*, 2006; Natanson *et al.*, 2006). However, for shortfin mako other studies have validated a biannual deposition rate in juveniles (Wells *et al.*, 2013; Kinney *et al.*, 2016). A study of several species showed that band pair deposition may be more related with somatic growth and vertebrae size than to time or age (Natanson *et al.*, 2018). Additionally, Harry (2018) alerts to the fact that many validation studies have reported underestimation in shark and ray ageing studies, especially in the larger and presumably older sharks. Ages can be underestimated if vertebrae cease to grow as maximum size is approached (Andrade *et al.*, 2019), therefore estimated maximum ages in this study should be considered as low estimates of maximum age for this species. Age validation through a species' lifespan is of extreme importance, as incorrect age and growth parameters will influence longevity, mortality estimates and other biological processes, which are important input parameters for stock assessments and fisheries management (Goldman *et al.*, 2012; Cailliet, 2015). Validation of band-pair deposition for *P. kamoharui* through its lifespan is lacking and should be considered in future studies.

In the present study, males and females reached different maximum sizes, but had similar maximum ages. The oldest estimated age was 13 years for males and 14 years for females. These estimates are older than the previous estimates by Lessa *et al.*

(2016) of 8 and 13 years for males and females, respectively, and Kindong *et al.* (2020) of 11 years for males and 10 years for females. The differences in the maximum estimated age could be related to differences in population or sampled areas and sizes but could also be related to differences in vertebrae processing. According to da Silva Ferrette *et al.* (2015) there is evidence for only one population in the Atlantic, and even between the Atlantic and the south-west Indian ocean, therefore differences can be due to the methodological aspects. The three available age and growth studies for crocodile shark have used different processing methods. In the current study vertebrae were sectioned and stained with crystal violet, while Lessa *et al.* (2016) used unstained sections and Kindong *et al.* (2020) used whole vertebrae stained with Alizarin Red S.

Contrary to the previous studies in age and growth for this species, that found no differences between males' and females' growth, in the present study differences were found between sexes, females having a higher L_{inf} and lower growth coefficients than males, for all tested models. Growth is similar up until 6 years old, when the growth curves begin to separate. Taking into consideration that the statistical fit, assessed by AIC and BIC, was best for the 2-parameter VBGF, this model was chosen as the model that best represents growth for this species. Sampling for smaller/younger specimens (see discussion above regarding size range) could help improve the growth curve fit in the initial years, especially for the 3-parameter VBGF that underestimated L_0 . It is noteworthy that other lamnoid sharks also present a lower L_{inf} and higher k for males than females (e.g. *Isurus oxyrinchus* (Rosa *et al.*, 2017), *Alopias superciliosus* (Fernandez-Carvalho *et al.*, 2015a), *Alopias vulpinus* (Gervelis & Natanson, 2013)).

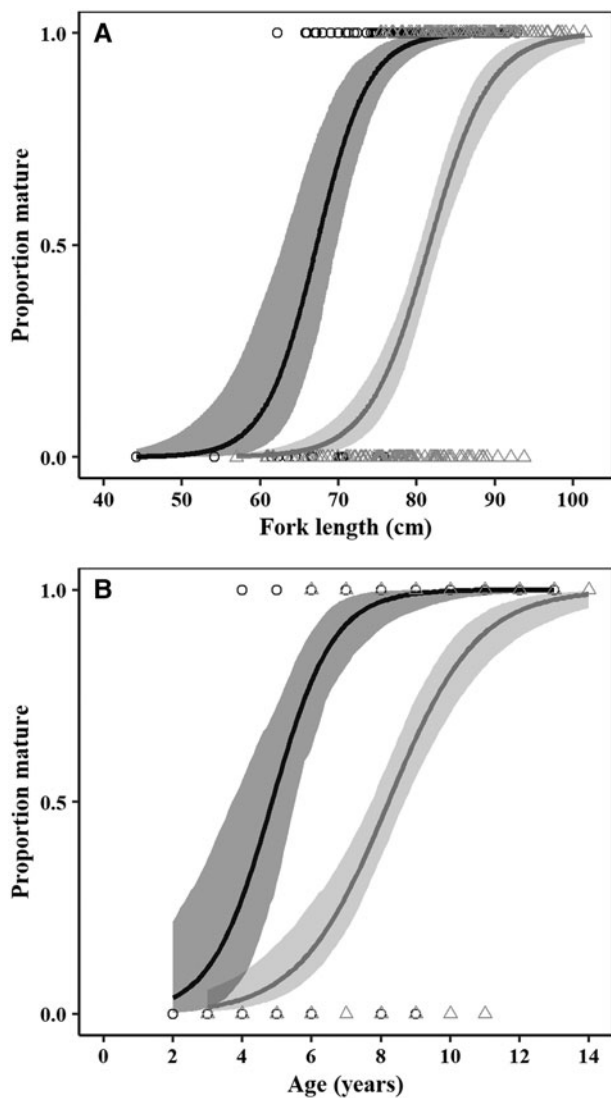


Fig. 8. (A) Size and (B) age-based maturity ogives for male (black) and female (grey) crocodile shark (*Pseudocarcharias kamoharai*), in the tropical Atlantic Ocean. Circles (○) and triangles (△) represent individual maturity data for males and females, respectively. The solid line represents the corresponding fitted logistic curve, while the shaded area represents the 95% confidence intervals.

Regarding trends in HSI and GSI between mature and immature specimens, Oliveira *et al.* (2010) found that in males there was no difference in HSI between maturity stages, while GSI increased with maturity. In the present study, the small sample of immature males with high variance in GSI, without separation of juvenile and maturing specimens, could have hindered the assessment of a significant increase in GSI once males mature. For females, Oliveira *et al.* (2010) had a more detailed analysis into the different maturity stages and found that in the early

stages of pregnancy there was an increase in HSI, while late-term pregnant females presented lower HSI, which recovered slightly in resting females. For GSI, the same authors observed that juvenile and resting female specimens had a low GSI, increasing in the initial pregnancy stages followed by a decrease towards late-term pregnancy. For the monthly analysis, the decrease in HSI in the months where GSI peaks, seems to agree with Oliveira *et al.* (2010) that noted a decrease in HSI through pregnancy, as females keep producing ova due to oophagy, spending high quantities of energy on this process. The same authors found all maturity stages throughout the year in females, with a peak in pregnant females occurring from May to July and juveniles in September and October. Both Oliveira *et al.* (2010) in the Atlantic Ocean and Fujita (1981) in the Pacific Ocean suggest that crocodile shark might have a prolonged mating and parturition season.

Maturity estimates from Indonesia (White, 2007) found males mature around 72.5 cm TL (61 cm FL) and females mature between 87 and 103 cm TL (74–88 cm FL). In the Atlantic, Oliveira *et al.* (2010) reported males mature between 76.0 and 81.0 cm TL (64–68 cm FL) and females L_{50} was estimated to be 91.6 cm TL (78 cm FL), while Wu *et al.* (2020) reports an L_{50} of 84.9 and 78.5 cm FL for females and males, respectively. In the current study maturity estimates for males (L_{50} = 67.2 cm FL) are similar to those reported by Oliveira *et al.* (2010) but lower than the estimates from Wu *et al.* (2020), while for females L_{50} (81.6 cm FL) is similar to both Oliveira *et al.* (2010) and Wu *et al.* (2020). Wu *et al.* (2020) notes that differences in maturity could be due to differences in fishing gear selectivity, but highlights that methodological differences in the critical values to define maturity can be a source of between-study variability in the proportion of mature individuals by size and, therefore, estimated L_{50} .

In terms of age-based maturity, our estimates of A_{50} for males (4.85 years) is higher than the age previously reported by Lessa *et al.* (2016) of 3.1 years but similar to the Kindong *et al.* (2020) estimates of 4.55 years. Regarding females, our current estimate of A_{50} of 8.21 years is higher than estimates in previous studies by Lessa *et al.* (2016) and Kindong *et al.* (2020) of 5.1 and 5.91 years, respectively. It should be noted that in the present study both size- and age-based maturity ogives were calculated directly using size, age and maturity data, while previous studies calculated length-based maturity ogives and then applied the growth equations to convert from size at maturity to age at maturity. Regardless of the differences in values, on all studies conducted so far females mature at greater lengths and ages than males. The same pattern exists in other lamniforms, with females maturing later than males (e.g. *Isurus oxyrinchus* (Natanson *et al.*, 2020), *Alopias superciliosus* (Fernandez-Carvalho *et al.*, 2015b), *Alopias vulpinus* (Natanson & Gervelis, 2013)).

Regarding fecundity, females were found to have mostly 4 embryos per reproductive cycle, but cases with 3 and 2 pups were also observed. This is similar to what has been reported by Oliveira *et al.* (2010), Dai *et al.* (2012) and Wu *et al.* (2020). The length of the reproductive cycle is not yet known for this

Table 3. Size and age maturity ogive for crocodile shark (*Pseudocarcharias kamoharai*) from the tropical Atlantic Ocean, fitted with individual observed data

Method	Sex	α	SE	β	SE	L_{50}	A_{50}	95% CI
Size-based	Males	-20.35	4.50	0.30	0.06	67.20		63.40–69.95
	Females	-20.93	2.99	0.26	0.04	81.57		80.21–82.94
Age-based	Males	-5.50	1.50	1.13	0.25		4.85	3.93–5.47
	Females	-6.42	1.05	0.78	0.12		8.21	7.78–8.71

The values of α and β are the estimated parameters of the logistic function, SE is the standard error for the parameters, L_{50} and A_{50} is the length (cm) and age (years) at 50% maturity, respectively, and the 95% bootstrapped confidence intervals (CI)

species, however, as discussed above, previous studies indicate that crocodile shark might have a prolonged reproductive season. Additionally, Oliveira *et al.* (2010) suggested that females might not be able to breed every year given the high expense of energy from the pregnant females during gestation. Further work to improve information on the reproductive cycle duration should be conducted, as this will influence estimates of how many litters, and therefore the overall number of pups a female can have during its mature lifespan.

This study adds to knowledge of important life-history characteristics of crocodile shark in the Atlantic Ocean that can be used to promote science-based fisheries management and conservation actions. Further work should focus on the validation of the band pair deposition rates and the duration of the reproductive cycle. Furthermore, fisheries management and conservation initiatives would greatly benefit from improvements in the recording and reporting of catch data, including discards.

Supplementary material. The supplementary material for this article can be found at <https://doi.org/10.1017/S0025315421000588>

Acknowledgements. Biological sampling for this study was carried out by IPMA through the National Program for Biological Sampling (PNAB), within the scope of the European Data Collection Framework (EU/DCF). The authors thank all skippers, crews and fishery observers who contributed with data and samples for this study. There was also support from FCT through project UIDB/04326/2020.

Financial support. D. Rosa is supported by an FCT Doctoral grant (Ref: SFRH/BD/136074/2018) through National Funds and the European Social Fund.

References

- Abramoff MD, Magalhaes PJ and Ram SJ (2004) Image processing with ImageJ. *Biophotonics International* **11**, 36–42.
- Andrade I, Rosa D, Muñoz-Lechuga R and Coelho R (2019) Age and growth of the blue shark (*Prionace glauca*) in the Indian Ocean. *Fisheries Research* **211**, 238–246.
- Ardizzone D, Cailliet GM, Natanson LJ, Andrews AH, Kerr LA and Brown TA (2006) Application of bomb radiocarbon chronologies to shortfin mako (*Isurus oxyrinchus*) age validation. *Environmental Biology of Fishes* **77**, 355–366.
- Ariz J, Delgado de Molina A, Ramos ML and Santana JC (2006) Check list and catch rate data by hook type and bait for bycatch species caught by Spanish experimental longline cruises in the south-western Indian Ocean during 2005. *Indian Ocean Tuna Commission (IOTC Document)*, IOTC-2006-WPBy-04, 10 pp.
- Ariz J, Delgado de Molina A, Ramos ML and Santana JC (2007) Length-weight relationships, conversion factors and analyses of sex-ratio, by length-range, for several species of pelagic sharks caught in experimental cruises on board Spanish longliners in the South Western Indian Ocean during 2005. *Indian Ocean Tuna Commission (IOTC Document)*, IOTC-2007-WPEB-04, 23 pp.
- Beamish RJ and Fournier DA (1981) A method for comparing the precision of a set of age determinations. *Canadian Journal of Fisheries and Aquatic Sciences* **38**, 982–983.
- Cailliet CM (2015) Perspectives on elasmobranch life-history studies: a focus on age validation and relevance to fishery management. *Journal of Fish Biology* **87**, 1271–1292.
- Cailliet GM, Smith WD, Mollet HF and Goldman KJ (2006) Age and growth studies of chondrichthyan fishes: the need for consistency in terminology, verification, validation, and growth function fitting. *Environmental Biology of Fishes* **77**, 211–228.
- Campana SE (2001) Accuracy, precision, and quality control in age determination, including a review of the use and abuse of age validation methods. *Journal of Fish Biology* **59**, 197–242.
- Canty A and Ripley B (2019) boot: Bootstrap R (S-Plus) Functions. R package version 1.3-22.
- Coelho R, Fernandez-Carvalho J, Lino PG and Santos MN (2012) An overview of the hooking mortality of elasmobranchs caught in a swordfish pelagic longline fishery in the Atlantic Ocean. *Aquatic Living Resources* **25**, 311–319.
- Compagno LJV (2001) Sharks of the world. An annotated and illustrated catalogue of shark species known to date. Volume 2. Bullhead, mackerel and carpet sharks (Heterodontiformes, Lamniformes and Orectolobiformes). *FAO Species Catalogue for Fishery Purposes*. Rome: FAO, No. 1, Vol. 2, 269 pp.
- Cortés E, Domingo A, Miller R, Forselleo R, Mas F, Arocha F, Camapana S, Coelho R, Da Silva C, Hazin FHV, Holtzhausen H, Keene K, Lucena F, Ramirez K, Santos MN, Semba-Murakami Y and Yokawa K (2015) Expanded ecological risk assessment of pelagic sharks caught in Atlantic pelagic longline fisheries. *Collective Volume of Scientific Papers ICCAT 71*, 2637–2688.
- Dai J, Zhu JF, Chen XJ, Xu LX and Chen Y (2012) Biological observations on the crocodile shark *Pseudocarcharias kamoharai*. *Journal of Fish Biology* **80**, 1207–1212.
- da Silva Ferrette BL, Mendonça FF, Coelho R, de Oliveira PGV, Hazin FHV, Romanov EV, Oliveira C, Santos MN and Foresti F (2015) High connectivity of the crocodile shark between the Atlantic and southwest Indian oceans: highlights for conservation. *PLoS ONE* **10**, e0117549.
- Elzhov TV, Mullen KM, Spiess A-N and Bolker B (2016) minpack.lm: R Interface to the Levenberg-Marquardt Nonlinear Least-Squares Algorithm Found in MINPACK, Plus Support for Bounds. R package version 1.2-1.
- Fernandez-Carvalho J, Coelho R, Erzini K and Santos MN (2015a) Modeling age and growth of the bigeye thresher (*Alopias superciliosus*) in the Atlantic Ocean. *Fishery Bulletin* **113**, 468–481.
- Fernandez-Carvalho J, Coelho R, Mejuto J, Cortés E, Domingo A, Yokawa K, Liu K-M, García-Cortés B, Forselleo R, Ohshimo S, Ramos-Cartelle A, Tsai W-P and Santos MN (2015b) Pan-Atlantic distribution patterns and reproductive biology of the bigeye thresher, *Alopias superciliosus*. *Reviews in Fish Biology and Fisheries* **25**, 551–568.
- Fujita K (1981) Oviparous embryos of the pseudocarchariid shark, *Pseudocarcharias kamoharai*, from the central Pacific. *Japanese Journal of Ichthyology* **28**, 37–44.
- Gervelis BJ and Natanson LJ (2013) Age and growth of the common thresher shark in the Western North Atlantic Ocean. *Transactions of the American Fisheries Society* **142**, 1535–1545.
- Goldman KJ, Cailliet GM, Andrews AH and Natanson LJ (2012) Assessing the age and growth of chondrichthyan fishes. In Carrier JC, Musick JA and Heithaus MR (eds), *Biology of Sharks and Their Relatives*, 2nd edn. Boca Raton, FL: CRC Press, pp. 423–451.
- Harry AV (2018) Evidence for systemic age underestimation in shark and ray ageing studies. *Fish and Fisheries* **19**, 185–200.
- Hazin FHV, Couto AA, Kihara K, Otsuka K and Ishino M (1990) Distribution and abundance of pelagic sharks in the south-western equatorial Atlantic. *Journal of the Tokyo University of Fisheries* **77**, 51–64.
- Kindong R, Wang H, Wu F, Dai X and Tian S (2020) Age, growth, and sexual maturity of the crocodile shark, *Pseudocarcharias kamoharai*, from the Eastern Atlantic Ocean. *Frontiers in Marine Science* **7**, 586024.
- Kinney MJ, Wells RJD and Kohin S (2016) Oxytetracycline age validation of an adult shortfin mako shark *Isurus oxyrinchus* after 6 years at liberty. *Journal of Fish Biology* **89**, 1828–1833.
- Kyne PM, Romanov E, Barreto R, Carlson J, Fernando D, Fordham S, Francis MP, Jabado RW, Liu K-M, Marshall A, Pacoureaux N and Sherley RB (2019) *Pseudocarcharias kamoharai*. In *The IUCN Red List of Threatened Species 2019*. e.T39337A2900108. Available from <https://www.iucnredlist.org/species/39337/2900108>.
- Lessa R, Andrade HA, De Lima KL and Santana FM (2016) Age and growth of the midwater crocodile shark *Pseudocarcharias kamoharai*. *Journal of Fish Biology* **89**, 371–385.
- Levene H (1960) Robust tests for equality of variances. In Olkin I, Ghurye SG, Hoefding W, Madow WG and Mann HB (eds), *Contributions to Probability and Statistics: Essays in Honor of Harold Hotelling*. Stanford, CA: Stanford University Press, pp. 278–292.
- Lilliefors HW (1967) On the Kolmogorov–Smirnov test for normality with mean and variance unknown. *Journal of the American Statistical Association* **62**, 399–402.
- Liu KM, Chiang PJ and Chen CT (1998) Age and growth estimates of the bigeye thresher shark, *Alopias superciliosus*, in northeastern Taiwan waters. *Fisheries Bulletin* **96**, 482–491.
- Liu KM, Chen CT, Liao TH and Joung SJ (1999) Age, growth, and reproduction of the pelagic thresher shark, *Alopias pelagicus* in the Northwestern Pacific. *Copeia* **1**, 68–74.

- Manly B** (2007) *Randomization Bootstrap and Monte Carlo Methods in Biology*, 3rd edn. New York, NY: Chapman & Hall/CRC.
- Natanson LJ and Gervelis BJ** (2013) The reproductive biology of the common thresher shark in the western North Atlantic Ocean. *Transactions of the American Fisheries Society* **142**, 1546–1562.
- Natanson LJ, Mello JJ and Campana SE** (2002) Validated age and growth of the porbeagle shark (*Lamna nasus*) in the western North Atlantic Ocean. *Fishery Bulletin* **100**, 266–278.
- Natanson LJ, Kohler NE, Ardizzone D, Cailliet GM, Wintner SP and Mollet HF** (2006) Validated age and growth estimates for the shortfin mako, *Isurus oxyrinchus*, in the North Atlantic Ocean. *Environmental Biology of Fishes* **77**, 367–383.
- Natanson LJ, Skomal GB, Hoffman SL, Porter ME, Goldman KJ and Serra D** (2018) Age and growth of sharks: do vertebral band pairs record age? *Marine and Freshwater Research* **69**, 1440–1452.
- Natanson LJ, Winton M, Bowlby H, Joyce W, Deacy B, Coelho R and Rosa D** (2020) Updated reproductive parameters for the shortfin mako (*Isurus oxyrinchus*) in the North Atlantic Ocean with inferences of distribution by sex and reproductive stage. *Fishery Bulletin* **118**, 21–36.
- Ogle DH, Wheeler P and Dinno A** (2020) FSA: Fisheries Stock Analysis. R package version 0.8.27.
- Oliveira P, Hazin FHV, Carvalho F, Rego M, Coelho R, Piercy A and Burgess G** (2010) Reproductive biology of the crocodile shark *Pseudocarcharias kamoharai*. *Journal of Fish Biology* **76**, 1655–1670.
- R Core Team** (2019) *R: A Language and Environment for Statistical Computing*. Vienna: R Foundation for Statistical Computing.
- Romanov E, Ward P, Levesque JC and Lawrence E** (2008) Preliminary analysis of crocodile shark (*Pseudocarcharias kamoharai*) distribution and abundance trends in pelagic longline fisheries. *Indian Ocean Tuna Commission (IOTC Document)*, IOTC-2008–WPEB-09, 29 pp.
- Rosa D, Mas F, Mathers A, Natanson LJ, Domingo A, Carlson J and Coelho R** (2017) Age and growth of shortfin mako in the North Atlantic, with revised parameters for consideration to use in the stock assessment. *International Commission for the Conservation of Atlantic Tunas (ICCAT SCRS Document)*, SCRS/2017/111, 22 pp.
- Stevens JD, Bonfil R, Dulvy NK and Walker PA** (2000) The effects of fishing on sharks, rays, and chimaeras (Chondrichthyans), and the implications for marine ecosystems. *ICES Journal of Marine Science* **57**, 476–494.
- Walsh WA, Bigelow KA and Sender KL** (2009) Decreases in shark catches and mortality in the Hawaii-based longline fishery as documented by fishery observers. *Marine and Coastal Fisheries: Dynamics, Management, and Ecosystem Science* **1**, 270–282.
- Wells RJD, Smith SE, Kohin S, Freund E, Spear N and Ramon DA** (2013) Age validation of juvenile shortfin mako (*Isurus oxyrinchus*) tagged and marked with oxytetracycline off southern California. *Fishery Bulletin* **111**, 147–160.
- White WT** (2007) Biological observations on lamnoid sharks (Lamniformes) caught by fisheries in eastern Indonesia. *Journal of the Marine Biological Association of the United Kingdom* **87**, 781–788.
- Wickham H** (2016) *ggplot2: Elegant Graphics for Data Analysis*. New York, NY: Springer.
- Wu F, Kindong R, Dai XJ, Sarr O, Zhu JF, Tian SQ, Li Y and Nsangué BTN** (2020) Aspects of the reproductive biology of the blue and crocodile sharks in the tropical Eastern Atlantic Ocean. *Journal of Fish Biology* **2020**, jfb.14526.